

# Communications

## Phase Relations in the System MgO-SiO<sub>2</sub>-ZrO<sub>2</sub> at 1700 K

S.S. PANDIT and K.T. JACOB

With an increasing demand for high-purity steels, pretreatment of hot metal is becoming more prevalent. Basically, sulfur, silicon, and phosphorus are removed during pretreatment. A low silicon level in the hot metal results in reduced slag volume and lower iron loss in the slag. In addition, refractory wear is reduced, and the life of the furnace lining is increased in basic oxygen steel-making practice. *In situ* chemical analysis of silicon is necessary for a better control of the desiliconization process. Several sensors for silicon have been proposed. The sensors are based on either a liquid silicate electrolyte,<sup>11-61</sup> or a solid ZrO<sub>2</sub>-based electrolyte with zircon as the auxiliary electrode.<sup>17,8,91</sup> ZrO<sub>2</sub>-based solid electrolyte sensors with an appropriate auxiliary electrode have several advantages relative to sensors based on liquid electrolyte. As discussed by Jacob *et al.*,<sup>101</sup> there are stability constraints in the design of galvanic cells using auxiliary electrodes.

A knowledge of phase relations in the ternary system MgO-SiO<sub>2</sub>-ZrO<sub>2</sub> is useful for selecting an appropriate auxiliary electrode in combination with MgO-stabilized zirconia. In this investigation, an isothermal section of the phase diagram of the system MgO-SiO<sub>2</sub>-ZrO<sub>2</sub> at 1700 K has been established by equilibrating mixtures of component oxides in air, followed by quenching and phase identification by optical microscopy, energy dispersive analysis of X-rays (EDAX), and X-ray diffraction analysis (XRD). Further, using known thermodynamic data on the condensed phases in the system, the phase relations have been computed by applying the method of free energy minimization to confirm the experimental findings.

The starting materials used in this investigation were powders of MgO, ZrO<sub>2</sub>, and SiO<sub>2</sub> (cristoballite), each of 99.99 pct purity. Air was dried by passing through columns containing silica gel, anhydrous magnesium perchlorate (Mg(ClO<sub>4</sub>)<sub>2</sub>), and phosphorus pentoxide (P<sub>2</sub>O<sub>5</sub>). The phase relations in the MgO-SiO<sub>2</sub>-ZrO<sub>2</sub> system were explored by equilibrating mixtures of the component oxides in dry air at 1700 K, followed by quenching and phase identification. The apparatus used for equilibrium studies was similar to that described elsewhere.<sup>111,121</sup> Precisely weighed quantities of the component oxides were thoroughly mixed either dry or with acetone, using an agate mortar and pestle. The intimate mixture was pressed into pellets at a pressure of 25 MPa using a steel die. The crucibles containing the samples were suspended in the even-temperature zone of a vertical furnace. Samples

were equilibrated for a total duration of 250 ks at 1700 K. The samples were quenched, ground to -325 mesh, and repelletized twice during this period. Part of the quenched sample was mounted and polished for examination by optical microscopy and scanning electron microscopy (SEM). A part of the sample was analyzed by XRD. In XRD, Cu K<sub>α</sub> radiation and Ni filters were used. To obtain good reproducibility by EDAX, the grain size had to be larger than 30 μm. Synthetic ZrO<sub>2</sub>, MgO, and ZrSiO<sub>4</sub> were used as standards.

The overall chemical compositions of the 27 samples examined in this study are shown in Figure 1. Of these, eight compositions lie on the three binaries CaO-ZrO<sub>2</sub>, ZrO<sub>2</sub>-SiO<sub>2</sub>, and CaO-SiO<sub>2</sub>, and the remaining 19 lie inside the ternary triangle. Phase identification in equilibrated samples was based on comparison with the published<sup>13-171</sup> diffraction patterns. The crystal structures, lattice parameters, and data sources for the compounds are listed in Table I. No ternary compounds were observed in this system at 1700 K. The isothermal section of the phase diagram for MgO-SiO<sub>2</sub>-ZrO<sub>2</sub> at 1700 K deduced from the results of this study is shown in Figure 1. On the MgO-ZrO<sub>2</sub> pseudobinary, the tetragonal and cubic solid solution phases are located at the ZrO<sub>2</sub>-rich end. In the MgO-SiO<sub>2</sub> pseudobinary, two compounds, Mg<sub>2</sub>SiO<sub>4</sub> and MgSiO<sub>3</sub>, have been identified. ZrSiO<sub>4</sub> was the only stable phase at 1700 K in the ZrO<sub>2</sub>-SiO<sub>2</sub> system. The equilibrium conjugation lines are shown in Figure 1. ZrO<sub>2</sub>-rich solid solutions along the MgO-ZrO<sub>2</sub> binary with tetragonal and cubic structures are in equilibrium with Mg<sub>2</sub>SiO<sub>4</sub>. ZrSiO<sub>4</sub> coexists with Mg<sub>2</sub>SiO<sub>4</sub> and MgSiO<sub>3</sub>.

Figure 1 clearly indicates that zircon is not the ideal auxiliary electrode for use with MgO-stabilized ZrO<sub>2</sub>, which is a good ionic conductor at high temperatures. Zircon is not phase compatible with MgO-stabilized zirconia. The solid-state reaction at the interface between the solid electrolyte and auxiliary electrode would alter the chemical potentials at the interface and thus effect the electromotive force (emf) response. From the thermodynamic point of view, Mg<sub>2</sub>SiO<sub>4</sub> is a suitable auxiliary electrode in conjunction with ZrO<sub>2</sub>-based solid solutions. To uniquely establish the activity of SiO<sub>2</sub> at the interface between the solid electrolyte and the auxiliary electrode, three-phase mixtures may be used. Partially stabilized zirconia, which contains a mixture of tetragonal and cubic solid solutions, in equilibrium with Mg<sub>2</sub>SiO<sub>4</sub> is a potential system with a well-defined activity of SiO<sub>2</sub>. However, the activity of SiO<sub>2</sub> is rather low in this phase field. Consequently, the equilibrium oxygen potential at the electrode-electrolyte interface would be lowered further, increasing electronic conduction in the solid electrolyte. Experimental trials are thus necessary to test the efficacy of Mg<sub>2</sub>SiO<sub>4</sub> as an auxiliary electrode with MgO-stabilized ZrO<sub>2</sub> in Si sensors. MgSiO<sub>3</sub> cannot be used as an auxiliary electrode since it does not coexist with phases exhibiting fast-ion conduction.

The experimental phase diagram for the system MgO-SiO<sub>2</sub>-ZrO<sub>2</sub> has been confirmed by computation using available thermodynamic data for the condensed phases. The free-energy minimization principle was used to identify the stable phase assemblies at 1700 K. Although the phase diagram for the binary system MgO-ZrO<sub>2</sub> has

S.S. PANDIT, Scientific Officer, Department of Metallurgy, and K.T. JACOB, Chairman and Professor, Materials Research Center, and Professor, Department of Metallurgy, are with the Indian Institute of Science, Bangalore 560012, India.

Manuscript submitted June 24, 1994.

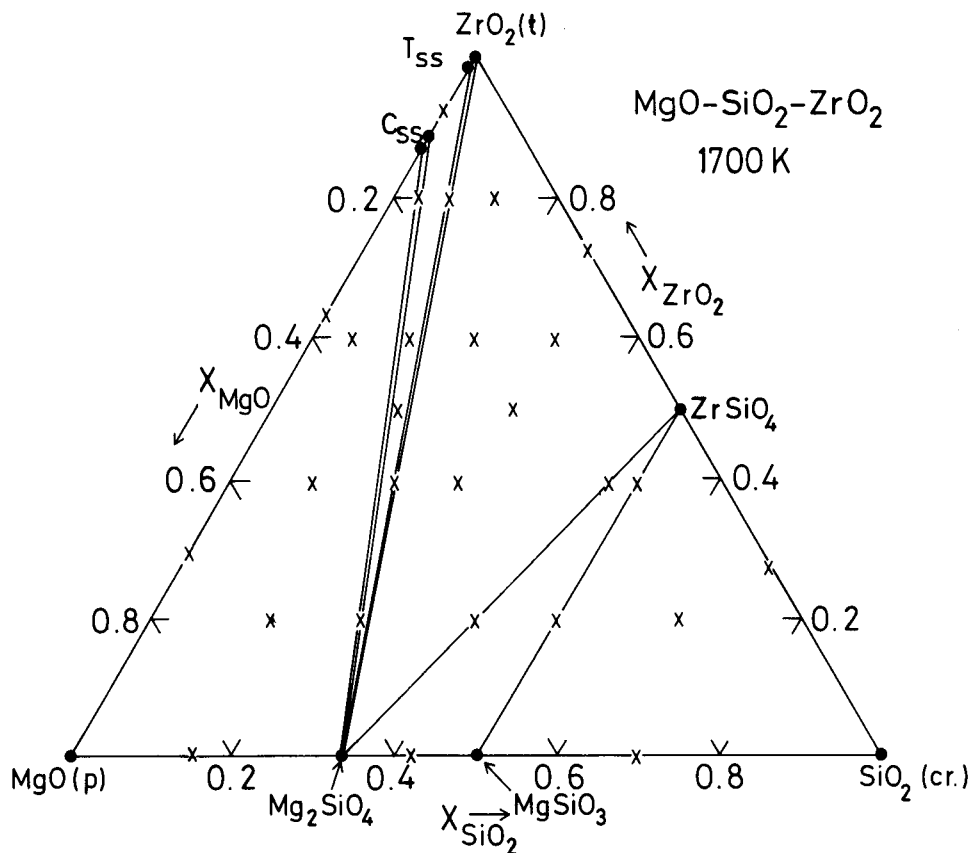


Fig. 1—Isothermal section of the ternary phase diagram for the system MgO-SiO<sub>2</sub>-ZrO<sub>2</sub> at 1700 K obtained in this study. The cross marks indicate the overall composition of the samples examined.

**Table I. Crystal Structure and Lattice Parameters of Condensed Phases in the System MgO-SiO<sub>2</sub>-ZrO<sub>2</sub>**

Compound	Lattice Parameter						Structure (Space Group)	Reference
	(nm)			(deg)				
	<i>a</i>	<i>b</i>	<i>c</i>	$\alpha$	$\beta$	$\gamma$		
ZrSiO <sub>4</sub> (Zircon)	0.471	—	1.045	—	—	—	tetragonal (I4 <sub>1</sub> /a)	13
MgSiO <sub>3</sub> (Enstatite)	1.823	0.884	0.519	—	—	—	orthorhombic (Pbca)	14, 15
MgSiO <sub>3</sub> (Clinoenstatite)	0.961	0.882	0.517	—	108.3	—	monoclinic (P2 <sub>1</sub> /c)	16
Mg <sub>2</sub> SiO <sub>4</sub> (Forsterite)	0.598	1.020	0.476	—	—	—	orthorhombic (Pmnb)	17

**Table II. The Standard Gibbs Free Energies of Formation and Mixing for Solid Phases in the System MgO-SiO<sub>2</sub>-ZrO<sub>2</sub> from Component Oxides at 1700 K**

Compound/Phase	Reference State for Binary Oxides	$\Delta G_f^\circ$ (kJ · mol <sup>-1</sup> )
ZrSiO <sub>4</sub> (Zircon)	ZrO <sub>2</sub> (tetragonal) SiO <sub>2</sub> (cristoballite)	-3.85
MgSiO <sub>3</sub> (Enstatite)	MgO (periclase) SiO <sub>2</sub> (cristoballite)	-27.80
Mg <sub>2</sub> SiO <sub>4</sub> (Forsterite)	MgO (periclase) SiO <sub>2</sub> (cristoballite)	-52.50
$\Delta G^M$ (kJ · mol <sup>-1</sup> )		
C <sub>ss</sub>	ZrO <sub>2</sub> (tetragonal) MgO (periclase)	$2.13 X_{ZrO_2} + 53.76 X_{MgO} + 14.13(X_{ZrO_2} \ln X_{ZrO_2} + X_{MgO} \ln X_{MgO}) + X_{ZrO_2} X_{MgO} [-33.45 + 1.56(X_{ZrO_2} - X_{MgO})]$
T <sub>ss</sub>	ZrO <sub>2</sub> (tetragonal) MgO (periclase)	$98.95 X_{MgO} + 14.13(X_{ZrO_2} \ln X_{ZrO_2} + X_{MgO} \ln X_{MgO}) - 36.13 X_{ZrO_2} X_{MgO}$

been investigated several times,<sup>118-231</sup> there is very little information on thermochemical properties of the condensed phases in the system. Recently Du *et al.*<sup>1241</sup> have presented an optimized set of thermodynamic parameters for the MgO-ZrO<sub>2</sub> binary by applying the CALPHAD<sup>125,261</sup> method to the experimental phase diagram and limited thermochemical data. The liquid and tetragonal solid solutions were described by the regular solution model, whereas for the cubic solid solution, a subregular solution model was used. The terminal solid solutions based on monoclinic-ZrO<sub>2</sub> and periclase-MgO were treated as pure oxides in view of the negligible solubilities. Their optimized thermochemical parameters were used in this study. In the ZrO<sub>2</sub>-SiO<sub>2</sub> binary, zircon (ZrSiO<sub>4</sub>) is the only stable phase reported in the literature. Rosén and Muan<sup>1271</sup> have measured the standard Gibbs energy of formation of ZrSiO<sub>4</sub>. However, there is some disagreement between their data and the phase diagram of Butterman and Foster.<sup>1281</sup> Recently, Jacob and Waseda<sup>1291</sup> have refined Rosén and Muan's data to fit the phase diagram. The optimized data of Jacob and Waseda for ZrSiO<sub>4</sub> is used in the present computation.

Robie *et al.*<sup>1301</sup> have measured the heat capacities and entropies of Mg<sub>2</sub>SiO<sub>4</sub> using an adiabatically shielded calorimeter in the temperature range 5 to 380 K. The heat capacity data is combined with the heat content data of Orr<sup>1311</sup> between 398 and 1808 K to generate values for the molar heat capacity and entropy of Mg<sub>2</sub>SiO<sub>4</sub> as a function of temperature. The enthalpies of formation of enstatite (MgSiO<sub>3</sub>) and forsterite (Mg<sub>2</sub>SiO<sub>4</sub>) from quartz and periclase-MgO were determined by Brousse *et al.*<sup>1321</sup> by solution calorimetry using a molten alkali borate as solvent. The new calorimetric data for enthalpy of formation of magnesium silicates supercede those suggested in the JANAF Tables.<sup>1331</sup> From the calorimetric data, the standard Gibbs energy of formation of Mg<sub>2</sub>SiO<sub>4</sub> was computed. Data for crystallographic transitions and the associated changes in thermodynamic properties of SiO<sub>2</sub> were taken from JANAF. The standard Gibbs energy of formation of MgSiO<sub>3</sub> was computed using the calorimetric data of Brousse *et al.*<sup>1321</sup> for enthalpy of formation and entropy data suggested in JANAF based on low-temperature heat capacity (53 to 295 K) measurements of Kelley<sup>1341</sup> and high-temperature (580 to 1570 K) studies of Wagner.<sup>1351</sup> The Gibbs free energies of formation of all the condensed phases in the system MgO-SiO<sub>2</sub>-ZrO<sub>2</sub> at 1700 K used in the present computation are listed in Table II. A free-energy minimization routine was used to identify the stable phase or phase mixtures at selected compositions. The computed results confirm the experimental findings.

In summary, the isothermal section of the phase diagram of the system MgO-SiO<sub>2</sub>-ZrO<sub>2</sub> at 1700 K has been established by equilibrating mixtures of component oxides in air followed by quenching and phase identification by optical microscopy, SEM with EDAX attachment, and XRD. Computations based on the free-energy minimization principle using available data confirm the experimental findings. The results indicate that zircon is not in thermodynamic equilibrium with magnesia-stabilized zirconia. For withstanding chemical interactions with FeO, (MgO)ZrO<sub>2</sub> is superior to (CaO)ZrO<sub>2</sub> ceramic. The silica-containing phase in equilibrium with

MgO-stabilized zirconia is Mg<sub>2</sub>SiO<sub>4</sub>. The use of Mg<sub>2</sub>SiO<sub>4</sub> as an auxiliary electrode in conjunction with zirconia-based solid solution would result in lower oxygen potential and enhanced electronic conductivity in the solid electrolyte. The viability of a silicon sensor based on (MgO)ZrO<sub>2</sub>/Mg<sub>2</sub>SiO<sub>4</sub> couple needs experimental verification.

## REFERENCES

- O.A. Esin and L.K. Gavrilov: *Izp. Akad. Nauk. SSSR, OTN*, 1951, vol. 8, pp. 1234-42.
- K. Schwerdtfeger and H.-J. Engell: *Arch. Eisenhüttenwes.*, 1964, vol. 35, pp. 533-40, 1027.
- K. Schwerdtfeger and H.-J. Engell: *TMS-AIME*, 1965, vol. 233, pp. 1327-32.
- T. Onoye, A. Egami, S. Nishi, and K. Narita: *Trans. Iron Steel Inst. Jpn.*, 1984, vol. 24, p. B-45.
- K. Ichihara, D. Janke, and H.-J. Engell: *Steel Res.*, 1986, vol. 57 (4), pp. 166-71.
- F. Buiarelli and P. Granati: *Steel Res.*, 1990, vol. 61 (2), pp. 60-63.
- M. Iwase: *Scand. J. Metall.*, 1988, vol. 17, pp. 50-56.
- D. Janke: *Solid State Ionics*, 1990, vols. 40-41, pp. 767-69.
- K. Raiber, S.W. Tu, and D. Janke: *Steel Res.*, 1990, vol. 61, pp. 430-37.
- K.T. Jacob, K. Swaminathan, and O.M. Sreedharan: *Solid State Ionics*, 1989, vol. 34, pp. 167-73.
- K.T. Jacob and T. Mathews: *J. Mater. Chem.*, 1991, vol. 1 (4), pp. 545-49.
- S.S. Pandit and K.T. Jacob: *Steel Res.*, 1994, vol. 65, in press.
- L. Liu: *Earth Planet Sci. Lett.*, 1979, vol. 44 (3), pp. 459-65.
- S.S. Pollack and W.D. Ruble: *Am. Mineral.*, 1964, vol. 49 (7-8), pp. 983-92.
- D.A. Stephenson, C.B. Selar, and J.V. Smith: *Mineral Mag.*, 1966, vol. 35 (273), pp. 838-46.
- U.S. National Bureau of Standards, Monograph No. 25, 1984, vol. 20, p. 89.
- U.S. National Bureau of Standards, Monograph No. 25, 1984, vol. 20, p. 71.
- R.C. Garvie: *High Temperature Oxides, Part II*, Academic Press, New York, NY, 1970, p. 117.
- S.M. Sim and V.S. Stubican: *J. Am. Ceram. Soc.*, 1987, vol. 70 (7), pp. 521-26.
- C.F. Grain: *J. Am. Ceram. Soc.*, 1967, vol. 50 (6), pp. 288-90.
- D. Vichniaki and V.S. Stubican: *J. Am. Ceram. Soc.*, 1965, vol. 48 (6), pp. 292-97.
- M.J. Bannister: *J. Am. Ceram. Soc.*, 1989, vol. 72 (1), p. 166.
- S.M. Sim and V.S. Stubican: *J. Am. Ceram. Soc.*, 1989, vol. 72 (1), p. 167.
- Y. Du, Z. Jin, and P. Hnang: *J. Am. Ceram. Soc.*, 1992, vol. 75, pp. 3040-48.
- L. Kaufman and H. Bernstein: *Computer Calculation of Phase Diagrams*, Academic Press, New York, NY, 1970.
- H.L. Lukas, E. Th. Henig, and B. Zimmermann: *CALPHAD*, 1977, vol. 1, pp. 235-36.
- E. Rosén and A. Muan: *J. Am. Ceram. Soc.*, 1965, vol. 48 (11), pp. 603-04.
- W.C. Butterman and W.R. Foster: *Am. Mineral.*, 1967, vol. 52, pp. 880-85.
- K.T. Jacob and Y. Waseda: *J. Am. Ceram. Soc.*, 1994, vol. 77, in press.
- R.A. Robie, B.S. Hemingway, and H. Takei: *Am. Mineral.*, 1982, vol. 67, pp. 470-82.
- R.L. Orr: *J. Am. Chem. Soc.*, 1953, vol. 75, pp. 528-29.
- C. Brousse, R.C. Newton, and O.J. Kleppa: *Geochim. Cosmochim. Acta*, 1984, vol. 48, pp. 1081-88.
- M.W. Chase, Jr., C.A. Davies, J.R. Downey, Jr., D.J. Frurip, R.A. McDonald, and A.N. Syverud: *JANAF Thermochemical Tables*, 3rd ed., *J. Phys. Chem. Ref. Data*, 1985, vol. 14, Suppl. 1, pp. 1473-75; 1489-91; 1673-77.
- K.K. Kelley: *J. Am. Chem. Soc.*, 1943, vol. 65, pp. 339-43.
- H. Wagner: *Z. Anorg. Allg. Chem.*, 1932, vol. 208, pp. 1-22.